VIII International Conference on Computational Plasticity
COMPLAS VIII
E. Oñate and D. R. J. Owen (Eds)

SIMULATED VOID GROWTH AND FAILURE IN AM60B MAGNESIUM TENSION SPECIMENS

Philip M. Gullett[*], Mark F. Horstemeyer[†], Amy M. Waters[‡], and Kyle F. Frazier[*]

[*] Department of Civil Engineering
Mississippi State University
Mississippi State, MS 39762, USA
e-mail: pmgullett@msstate.edu

[†] Department of Mechanical Engineering
Mississippi State University
Mississippi State, MS 39762, USA

[‡]Lawrence Livermore National Laboratory
Livermore, CA 95370

Key words: Computational Plasticity, Damage progression, Voids

1 INTRODUCTION

In an effort to further reduce the weight of production vehicles, the automotive industry has exhibited a strong interest in the use of cast magnesium alloys for fabrication of lightweight structural components. Magnesium alloys are strong candidates due to excellent strength-to-weight ratio, castability, and machinablity. The porosity levels common in cast magnesium parts require a detailed understanding of the effects of porosity and damage on part performance in typical overload situations. It is well known that damage progression in materials under monotonic loading is due to nucleation, growth and coalescence of voids[1]. In materials with large porosity levels in highly stressed regions, the growth and coalescence of voids may be the determining factor in part failure. This study compares damage evolution observed via x-ray computed tomography in a monotically loaded AM60B notched bridgeman tensile specimen with damage evolution predicted in finite element simulations.

2 CAST MATERIAL AND MECHANICAL TESTING

The die cast AM60B magnesium alloy composition is Al-5.67%, Zn-0.15%-Zn, Si-0.377%, Fe-0.0011%, Cu-0.0035%, Ni-0.0001%, Ca-0.0033%. The specimens used in the study were cold chamber die cast with a injection temperature of 675-670 ºC, metal temperature of 750 ºC, and a die temperature of 300 ºC. Several of the notch tension specimens were submitted for standard mechanical testing, and the average mechanical properties are shown in Table 1.

Tensile strength	Yield strength	Elongation to failure	Elastic Modulus	Poisson's ratio	Density g / mm^3	UTS
220 MPa	130 MPa	6%	45 GPa	0.35	0.0018	241 MPa

Table 1 : Average material properites

3 COMPUTED TOMOGRAPHY

Tensile bar porosity was imaged using an X-ray tomographic microscope at the Stanford Synchrotron Radiation Laboratory (SSRL) [2]. The images resolved with a voxel size of 0.024×0.024×0.024 mm. Computed tomography scans were performed after 60, 87, 93, and 95% of the average failure loads listed in Table 1. The left-hand side of Figure 1 shows an example slice of porosity data. Scan data revealed porosity scattered in a random fashion within the sample as well as clearly defined flow lines – a cylindrical region of high porosity along the specimen axis. The flow lines are caused typically by a failure of molten streams of metal to merge. CT data analysis included quantification of void size distribution, nearest neighbor distances, void shape analysis and void growth.

4 NUMERICAL MODELING

The numerical simulation of the tensile response was designed to correlate directly with a particular notch tension specimen. Therefore, in addition to specifying geometry, boundary conditions and material response, the level and distribution porosity was initialized.

The cylindrical notch tensile specimen was geometrically represented by a quarter-space, axially symmetric model. The analysis was performed with ABAQUS software and utilized reduced integration, four-node, axisymmetric quadrilateral elements. Boundary conditions included uniform quasi-static axial extension along the top edge, symmetry along the specimen axis and bottom edge, and a traction free surface on the notch edge.

The material constitutive response was modeled using the Bammann-Johnson-Chiesa (BCJ) plasticity-damage model[3]. The BCJ is an internal state variable formulation that includes kinematic hardening, isotropic hardening, and damage rate as evolving state variables.

Damage (volume fraction of material within a continuum element) evolution is motivated by the Cock-Ashby[4] model of spherical void growth in a plastic material,

$$\dot{\varphi} = \left[\frac{1}{(1-\varphi)^m} - (1-\varphi) \right] \sinh\left[\frac{2(2m-1)p}{(2m+1)\bar{\sigma}} \right], \tag{1}$$

where φ is the volume fraction of porosity, p is the tensile pressure, $\bar{\sigma}$ the effective stress, and m is a void growth constant.

The BCJ model parameters were calibrated to the behavior of AM60B using a wide range of experimental data including tension, torsion, and reverse yield test data. The void growth constant m was determined using micromechanical finite element simulations[5].

4.1 Damage initialization

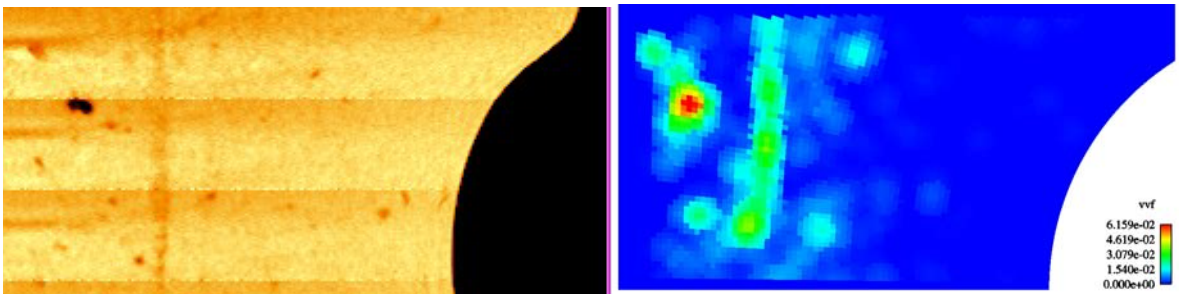

Figure 1: CT porosity data and initial porositie levels (vvf) in finite element mesh.

The damage state was initialized on a per element basis using data extracted from CT scans. CT scan data was averaged axially and was mapped to the finite element mesh using a moving least-squares fitting technique. The right hand side of Figure 1 shows a scan of the initial element porosities from the data mapping. The chief characteristics of the porosity include a single large pore in the upper left of the specimen, and a distinct cylindrical band of porosity running along the axis.

5 RESULTS AND DISCUSSION

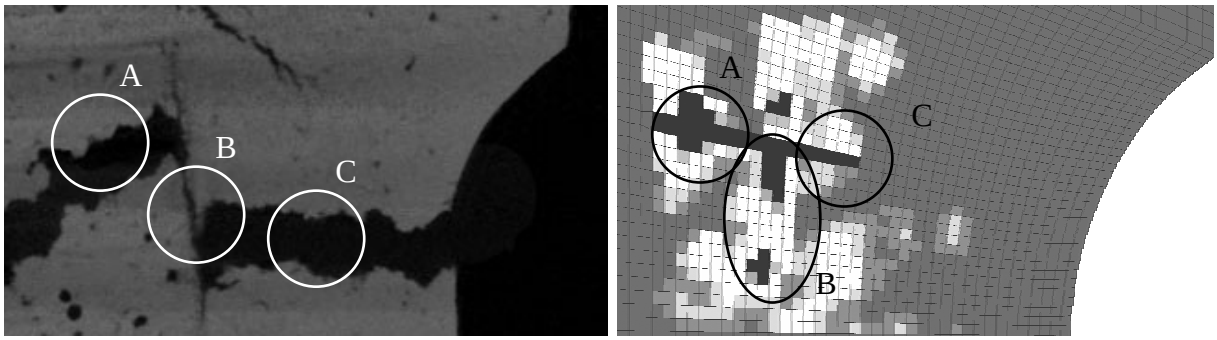

Figure 2: Fractured speciment and predicited damage from the finite element simulation. The black regions in the simulation represent element failures due to damage evolution.

Stress triaxiality is the primary driving factor for void growth in porous materials. In a uniform material, the notch geometry induces a smooth stress triaxiality field with a maximum value near the center of the specimen. In a damaged medium, stress concentrations induced by the presence of pores, may cause local regions of high stress triaxiality. As a result, void growth occurs where the combined damage and stress triaxialty synergize. The simulations as well as the damaged samples demonstrate this trend. The left-hand side of Figure 2 shows the fractured section of the failed sample, and the right-hand side shows predicted damage state. Three aspects of this failure are captured by the simulation. Area A shows that the fracture passes through the region with high initial porosity levels. The simulation predicted maximum void growth and initial failure in this region. Area B shows an axial fracture along the porous flow line. This fracture connects the region of high initial

porosity, A, with the region of highest stress triaxiality, C. Failure along the porous flow line was typical of all tested magnesium bars. Area C shows the radial fracture path across the specimen section in the region of high stress triaxiality. The simulations capture the observed damage evolution noted for Areas B and C. Significant axial void growth was predicted in Area B as evidenced by the failed and near failed elements along the flow line. Void growth in this area continued after the initial element failure in the large pore. After initial element failure occurs at the large pore, damage progresses radially both toward the specimen center and the notch edge. This predicted failure mode is evidenced by the failed elements aligned radially.

This study demonstrates a method of analysis that combines x-ray computed tomography, micromechanical finite element simulations and macro-scale continuum simulation based evaluation of damage evolution. Based on these initial findings, a strong collaboration of simulation with x-ray tomography results for the failure of notch tension specimens under monotonic loading is apparent.

6 CONCLUSIONS

- Damage progression in an AM60B notch tension specimen was quantified using x-ray computed tomography and finite element based simulation that includes and internal state variable representing void growth.
- The correlation between the observed results and the simulation predictions provides a basis for increased confidence in finite-element based analyses.

REFERENCES

[1] W.M. Garrison and N.R. Moody, “Ductile fracture”, J. Phys. Chem. Solids., **48**, 1035-1074 (1987)

[2] A.M. Waters, H.E. Martz, K.W. Dolan, M.F. Horstemeyer and R.E. Green, “Three dimensional void analysis of AM60B magnesium alloy tensile bars using computed tomography imagery”, Materials Evaluation, **58**, 1221-1227 (2000).

[3] M.F. Horstemeyer and A.M. Gokhale, “A void-crack nucleation model for ductile metals”, Int. J. Solids and Structures, **36**, 5029-5055 (1999).

[4] C.F. Cocks and M.G. Ashby, “Intergranular fracture during power-law creep under multiaxial stresses”, Metal Sci., **14**, 395-402 (1980).

[5] M.K. Jones, *Multi-Scale Analysis of Void Coalescence in Ductile Metals*, Masters Thesis, Mississippi State University (2005).